ACS Catalysis

Research Article

Cite This: ACS Catal. 2019, 9, 8835–8842

pubs.acs.org/acscatalysis

Oxa- and Azabenzonorbornadienes as Electrophilic Partners under Photoredox/Nickel Dual Catalysis

Youran Luo,[†,‡] Álvaro Gutiérrez-Bonet,[†] Jennifer K. Matsui,[†] Madeline E. Rotella,[§] Ryan Dykstra,[§] Osvaldo Gutierrez,*[,§] and Gary A. Molander*[,†]

[†]Roy and Diana Vagelos Laboratories, Department of Chemistry, University of Pennsylvania, 231 South 34th Street, Philadelphia, Pennsylvania 19104-6323, United States

[‡]Wuyuzhang Honors College, 29 Wangjiang Road, Chengdu, Sichuan 610064, China

[§]The Department of Chemistry and Biochemistry, University of Maryland, 0107 Chemistry Building, 8051 Regents Drive, College Park, Maryland 20742, United States

Supporting Information

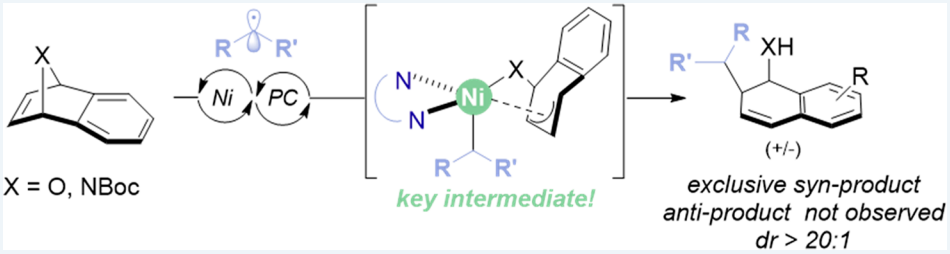

ABSTRACT: Herein, the introduction of oxa- and azabenzonorbornadienes into photoredox/nickel dual catalysis in a regioselective and diastereoselective transformation is disclosed. The inherent advantages of this dual catalytic system allow the use of alkyl motifs forming exclusively *cis*-1,2-dihydro-1-naphthyl alcohol backbones using readily accessible 4-alkyl-1,4-dihydropyridines (DHPs). Whereas previous studies have emphasized the use of nucleophilic organometallic coupling partners, this protocol grants access to a rather unexplored core featuring alkyl residues, while avoiding the use of highly reactive organometallic species (i.e., M = Al, Mg, Li, Zn, Zr). Density functional theory (DFT) calculations support an oxidative addition/reductive elimination mechanism, followed by a Curtin−Hammett scenario that controls the regioselectivity of the process, unlike previously reported transformations that proceed via a carbometalation/β-oxygen elimination mechanism.

KEYWORDS: *oxabenzonorbornadiene, Curtin−Hammett, photoredox/nickel dual catalysis, 4-alkyldihydropyridines, cross-coupling, regioselective*

INTRODUCTION

Building molecular complexity swiftly is the key to success in multiple disciplines that build upon organic synthesis knowledge (i.e., drug discovery, crop protection, dye development, biochemistry, material science, total synthesis).[1] However, to guarantee the implementation of new methods, the starting materials must be readily available, the retrosynthetic logic must be clear, and the reaction conditions must ensure good functional group tolerance.[2] Furthermore, molecular complexity is not to be limited to the introduction of new entities or functional groups within a molecule but could also be achieved by increasing its 3D-character. Along these lines, there is a great interest in introducing C(sp^3)-hybridized centers within molecules to explore new chemical space, given that sp^3-hybridized carbon atoms bestow a higher 3D-spatial geometry, which is associated with a higher ratio of success in the development of pharmaceutical drugs.[3]

Transition metal-catalyzed cross-coupling reactions have proven themselves unparalleled when forging new C−C bonds efficiently.[4] Among the multiple cross-coupling platforms, photoredox/nickel dual catalysis perfectly fulfills the aforementioned needs.[5] Such catalytic systems are efficient at room temperature, and usually, no highly reactive additives (i.e., strong bases or acids, oxidants, reductants) are needed. More importantly, because the reaction is based on radical partners, C(sp^3)-centered motifs are easily introduced. However, because of the nature of most of the electrophiles employed [i.e., aryl/vinyl (pseudo)halides], the bonds forged with this strategy are often limited to C(sp^3)−C(sp^2) centers, thus once again limiting the chemical space that can be accessed.[6]

In this vein, oxa- and azabenzonorbornadienes were examined as electrophilic partners[7] in a photoredox/nickel dual catalytic process, because upon reaction, a new regioselective C(sp^3)−C(sp^3) bond would be forged, resulting in the formation of 2-alkyl-1,2-dihydronaphthalenols. Such backbones are common intermediates in the preparation of

Received: June 14, 2019
Revised: August 9, 2019
Published: August 28, 2019

Downloaded via UNIV OF MARYLAND COLG PARK on February 4, 2020 at 16:40:53 (UTC).
See https://pubs.acs.org/sharingguidelines for options on how to legitimately share published articles.

© 2019 American Chemical Society

DOI: 10.1021/acscatal.9b02458
ACS Catal. 2019, 9, 8835–8842

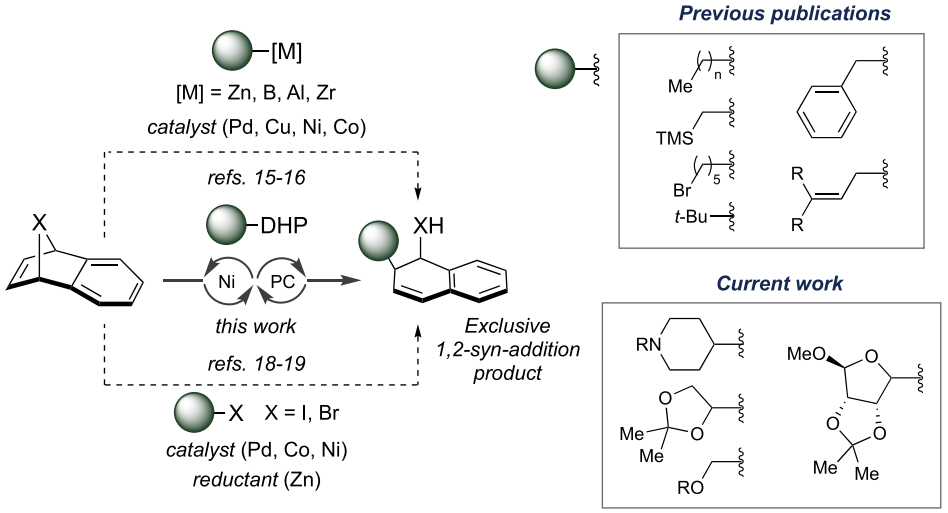

Figure 1. Ni/photoredox dual catalysis as a strategy to overcome previous limitations of the alkylation of oxa- and azabenzonorbornadienes.

Group II C-aryl glycoside antibiotics.[8,9] They have also been used as key intermediates in the total synthesis of podophyllotoxins (cancer chemotherapy drugs) by the Sherburn group[10] and as ligands.[11] Furthermore, these substructures can be easily modified (e.g., by oxidation, dehydration, hydrogenation, arylation), enabling the preparation of numerous distinct compounds from one common intermediate.[12]

Oxabenzonorbornadienes are characterized by the possession of an aromatic ring fused to a furan and a cyclohexene, and they can be easily accessed in one step from a [4 + 2]-cycloaddition between a furan derivative and a benzyne precursor.[13] There are numerous literature reports regarding the enantioselective transition metal-catalyzed ring opening of these entities with distinct nucleophiles (i.e., hydrides, alcohols, amines) to form a new C(sp^3)−heteroatom bond.[7] Notably, previous methods reported for the formation of alkyl C(sp^3)−C(sp^3) bonds rely heavily on using reactive organometallic reagents both with and without transition metal catalysis.

For example, the uncatalyzed alkylative ring opening is achieved with organolithium reagents[14] and leads to the *syn*-alkylated product upon exclusive exo-attack of the nucleophile. On the other hand, less reactive organometallic species, most notably organozinc reagents, react slowly in the absence of a metal catalyst and, therefore, have been widely employed in conjunction with palladium catalysts and chiral ligands for desymmetrization strategies, leading to diastereoselective and enantioenriched products.[15] Furthermore, asymmetric reports using other transition metal catalysts (i.e., Ni, Cu, and Co) and organometallic species (Zr, Al, and B) are known.[16] Despite the exceptional levels of enantiocontrol achieved in these cross-coupling reactions, most of these studies rely on dialkylzinc species, where one of the alkyl residues is not coupled with the substrate. Although with simple dialkylzinc species this is a minor limitation, in the context of complex alkyl motifs prepared via multistep sequences, it would become a considerable handicap. Furthermore, in almost all these cases, the alkyl motif is limited to benzylic, allylic, and simple hydrocarbon chains (Figure 1).[15,16]

anti-Selectivity has been observed mainly using systems based on copper catalysts.[17] From a mechanistic standpoint, the origin of this *anti*-selectivity remains elusive, with several mechanisms proposed.[17] On the contrary, the mechanism for the formation of the *syn* product under palladium catalysis is well understood.[15] Empirical evidence as well as quantum mechanical studies support a mechanism consisting of the initial formation of an organopalladium species that undergoes *syn*-carbopalladation followed by a β-oxygen elimination step.[15]

To avoid the use of organometallic species, aryl halides have been used as electrophiles in a reductive cross-coupling. However, detrimental superstoichiometric metallic reductants are required in these transformations.[18] In 2015, the Cheng group reported the first coupling of oxabenzonorbornadienes using alkyl halides in the presence of a nickel catalyst and zinc as a reductant.[19] Unfortunately, low yields were obtained in these reductive cross-couplings because of the decomposition of the oxabenzonorbornadiene. Nonetheless, Cheng's work avoids the use of organometallic species (a major limitation of the previous reports) and, thus, allowed greater functional group tolerance and an increase in molecular complexity within the alkyl motifs used.

Considering the precedented literature,[20] a more efficient alkylative event was anticipated using photoredox/nickel dual catalysis, where neither organometallic reagents nor high temperatures or stoichiometric reductants are required, allowing an expansion of the scope for this strategy in terms of oxabenzonorbornadiene stability, functional group tolerance, and molecular complexity.

RESULTS AND DISCUSSION

Encouraged by the potential synthetic applications of the proposed photoredox/Ni dual-catalyzed alkylation, identification of the best radical precursor was explored. In this type of transformation, 4-alkyl-1,4-dihydropyridines (DHPs) have previously been proven valuable in photoredox/nickel catalytic systems for the introduction of secondary or activated primary alkyl radicals in aryl- and heteroaryl motifs.[6c,21] More importantly, saccharyl-DHPs can be easily prepared and funneled into dual catalytic protocols, delivering nonclassical, arylated C-saccharides.[21c] In the present case, the combination of saccharyl-DHP radical precursors with epoxynaphthalene electrophiles would translate into a straightforward synthesis of Group II C-aryl glycoside antibiotics which, to date, have limited synthetic routes available, all of them involving the use of organometallic reagents.[8,9]

DOI: 10.1021/acscatal.9b02458
ACS Catal. 2019, 9, 8835−8842

Conceptually, alkylation of the oxa- and azabenzonorbornadienes poses several challenges, including the various regio- and stereochemical scenarios available (1,2- and 1,4-addition products,[22] as well as *syn*/*anti*-stereoisomers). However, a judicious choice of the ancillary ligand for the nickel catalyst was anticipated to lead to a satisfactory and useful product distribution.

On the basis of previously developed conditions,[21] the following was established: $NiCl_2$·dme as the precatalyst, acetone as the solvent, and 2,4,5,6-tetra-9*H*-carbazol-9-yl-1,3-benzenedicarbonitrile (4-CzIPN) as the photocatalyst. The latter was used in consideration of its proven ability to photocleave DHPs efficiently and its lower cost compared to other metal-based photocatalysts.[21] Anticipating the key role played by the ligand, screening was undertaken with an array of different nitrogen-based ligands. Diimine ligand **L1** outperformed all other ligands tested (Table 1, entry 1), even the prominently used dtbbpy and dMeObpy (entries 6 and 7),[21] delivering quantitative yields with excellent regio- and diastereocontrol.[23] To confirm the structure of the product, a suitable crystal was analyzed by X-ray diffraction, validating the regio- and stereochemistry of product **3a**. Notably, the reaction proceeds in the absence of ligand, although in dramatically lower yields (entry 2), but neither the regioselectivity nor the stereoselectivity was affected under these conditions. On the other hand, nickel is required, thus ruling out a free radical addition pathway.[24] Other solvents were deleterious for the reaction outcome (entries 8−10). We were interested in the role played by the pyridinium ion generated upon oxidative photolysis of the DHP; thus, different bases were tested (entries 12−13). Virtually no product was observed under these conditions, indicating that protonation of the resulting alkoxide by the pyridinium salt is crucial for catalytic turnover. Finally, lower Ni/L ratios diminished the overall yield (entry 1 vs 14). Notably, less rigid **L2** behaved similarly to **L1** (entry 14 vs 16). Finally, expecting a challenging coordination between the ligand and the nickel center to be responsible for the loss in reactivity at lower Ni/L ratios, we prepared and isolated the complex $NiCl_2$·**L1**. Under these conditions, low yields were still observed (entry 15). The reason for this remains unclear, but decomposition of the ligand or the fact that two equivalents of ligand are required to form a more stable tetracoordinated nickel(0) complex may be contributing factors.[25]

Table 1. Optimization of Reaction Conditions[a]

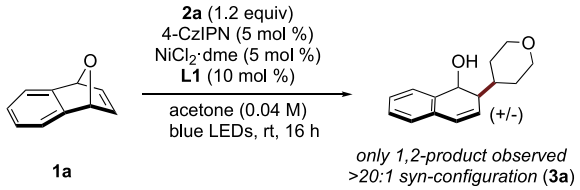

1a

only 1,2-product observed
>20:1 syn-configuration (**3a**)

entry	*deviation from standard conditions*	*NMR yield*
1	none	95 (92)
2	no **L1** was added	55
3	in the dark	*n.d.*
4	no $NiCl_2$•dme was added	*n.d.*
5	no 4-CzIPN was added	*n.d.*
6	using dtbbpy as ligand (7.5 mol %)	58 (55)
7	using dMeObpy as ligand (7.5 mol %)	68
8	using CH_3CN instead of acetone	38
9	using DMF instead of acetone	14
10	using THF instead of acetone	12
11	using $NiBr_2$·dme instead of $NiCl_2$·dme	62
12	adding lutidine (2.0 equiv) as base	16
13	adding Cs_2CO_3 (2.0 equiv) as base	*trace*
14	using **L1** (7.5 mmol %)	78
15	using $NiCl_2$•**L1** complex (5 mol %)	62
16	using **L2** (7.5 mmol %)	77 (75)

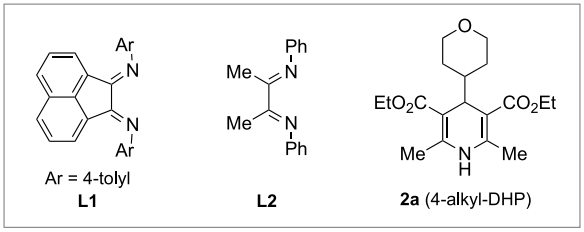

[a]Reaction conditions: **1a** (0.1 mmol), **2a** (0.12 mmol), 4-CzIPN (5 mol %), $NiCl_2$·dme (5 mol %), **L1** (10 mol %), acetone (2.5 mL, 0.04 M), blue LEDs, rt, 16 h. NMR yield uses diethyl fumarate as the internal standard. Numbers in brackets indicate isolated yields.

Since suitable reaction conditions were developed, the versatility of the present method in a variety of different scenarios was explored. First, we focused on studying different 4-alkyl-DHPs (Table 2). In general, secondary and stabilized primary radicals were successfully coupled with oxo- and azabenzonorbornadienes **1a**−**b**, while tertiary radicals failed to deliver the desired product. Secondary radicals, including heterocycles (**3a**,**c**,**j**), bicyclic structures (**3d**), and masked diols (**3e**), could be introduced in good to high yields. Likewise, primary radicals, including α-silyloxy (**3f**−**g**,**l**) and benzylic (**3h**−**i**) motifs, were coupled efficiently. In all cases, regardless of the nature of the radical, only the *syn*-1,2-addition product was observed. Notably, the reaction was not limited to epoxynaphthalenes, as azabenzonorbornadienes were suitable substrates as well, affording only the *syn*-1,2-addition product (**3j**−**l**). Importantly, despite the inherent propensity of the alcohol products to undergo dehydration,[14b,c] the mild reaction conditions prevented this decomposition pathway.

Intrigued by the excellent regio- and diastereocontrol observed, we examined diverse epoxynaphthalene cores to determine whether substrate control could be tuned on the basis of steric or electronic factors. Regardless of the substituents on the aromatic ring, exclusive *syn*-1,2-addition was observed (Table 3). However, in unsymmetrically substituted systems (**3q**/**3q**′), an almost 1:1 mixture of the two possible regioisomers was observed. The poor regioselectivity observed in this case is likely because of the ineffective steric effect of the distal substituent and the scarce electronic differentiation of the two bridgehead positions [σ_{meta} (**Cl**) 0.37 vs σ_{para} (**Cl**) 0.23],[26] which renders the nickel catalyst unable to discriminate between the two possible reaction sites.

Substitution on the cyclohexene motif did not hamper the reaction. As a general trend, when a substituent was located on position 2 (vinyl substituent), the alkyl residue was incorporated adjacent to it (**3r**,**t**−**u**). However, the formation of a quaternary center was observed in 22% yield for substrate **3s**. When comparing products **3s**−**u**, they all originate from the same epoxynaphthalene (**1h**). Therefore, the nature of the alkyl residue appears to dictate the regioselectivity. In this

DOI: 10.1021/acscatal.9b02458
ACS Catal. 2019, 9, 8835−8842

Table 2. Merging Oxa- and Azabenzonorbornadienes with 4-Alkyl-DHPs: Alkyl Radical Scope[a]

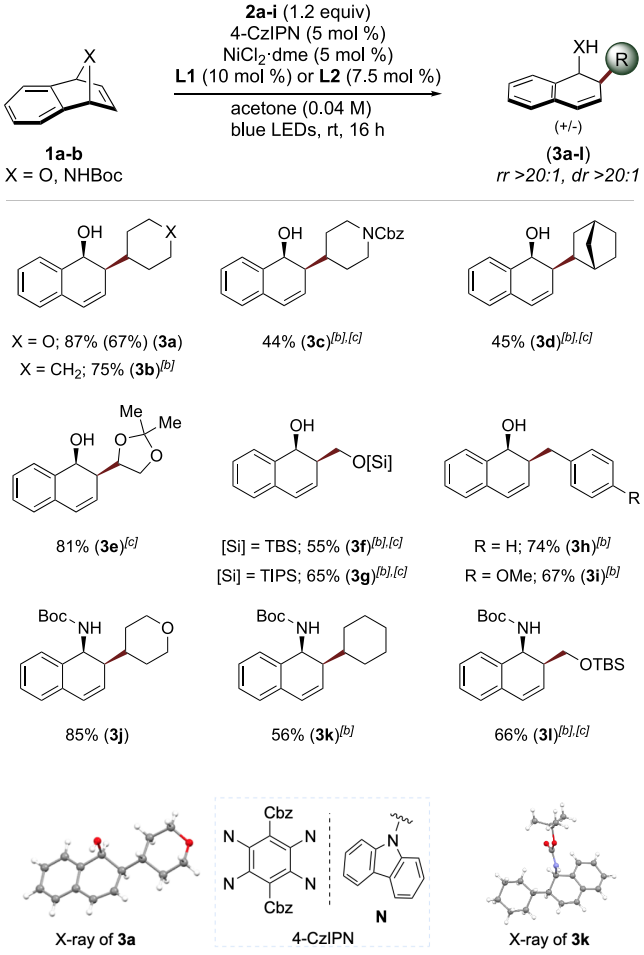

[a]Reaction conditions: **1** (0.5 mmol), **2** (1.2 equiv), 4-CzIPN (5 mol %), $NiCl_2$·dme (5 mol %), **L1** (10 mol %), acetone (0.04 M), blue LEDs, rt, 16 h. Yield in brackets represents a 5.0 mmol (**1a**) scale reaction. [b]Using **L2** (7.5 mol %). [c]Using **2** (1.5 equiv).

particular case, the quaternary product was only observed with the less sterically hindered primary benzylic radical, whereas for the more sterically encumbered secondary pyranyl and furanyl radicals, steric effects raise the transition state energy and inhibit reductive elimination (vide infra).

Mono- or disubstitution on the bridgehead position did not affect the relative *syn*-configuration between the hydroxyl group and the new alkyl motif introduced (**3v**–**3y**). Notably, when only one bridgehead position was occupied, the formation of the secondary alcohol was favored (**3v**, **3y**). On the other hand, in the presence of dissimilar substituents, the reaction favored the formation of the most stable alkene (**3w**).

A series of experimental mechanistic studies was carried out to gain further insights into the observed regioselectivity and diastereoselectivity. First, the pyridinium ion generated upon oxidative cleavage of the DHP was studied to determine if it was able to activate the epoxynaphthalene (**I**). However, when pyridinium·TFA **4** was added to epoxynaphthalene **1a**, no significant shift of the proton signals was observed, thus ruling out activation of the substrate by the byproduct (Figure 2, top). Next, the effect of the electronic nature of the alkyl radical motif was examined (Figure 2, bottom). To this end, a

Table 3. Merging Oxa- and Azabenzonorbornadienes with 4-Alkyl-DHPs: From Functional Group Influence to the Synthesis of Aryl C-Glycosides[a]

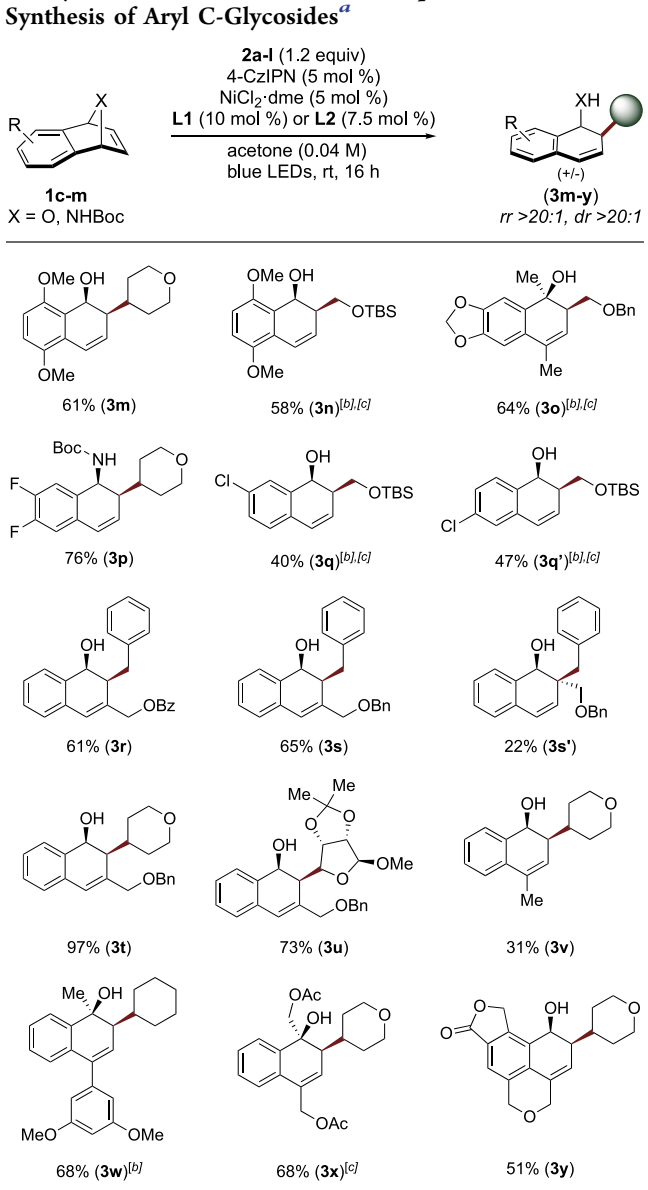

[a]Reaction conditions: **1** (0.5 mmol), **2** (1.2 equiv), 4-CzIPN (5 mol %), $NiCl_2$·dme (5 mol %), **L1** (10 mol %), acetone (0.04 M), blue LEDs, rt, 16 h. [b]Using **L2** (7.5 mol %). [c]Using **2** (1.5 equiv).

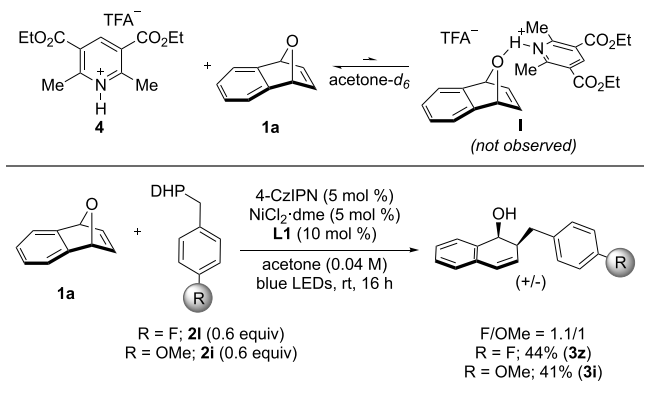

Figure 2. Mechanistic probes.

DOI: 10.1021/acscatal.9b02458
ACS Catal. 2019, 9, 8835−8842

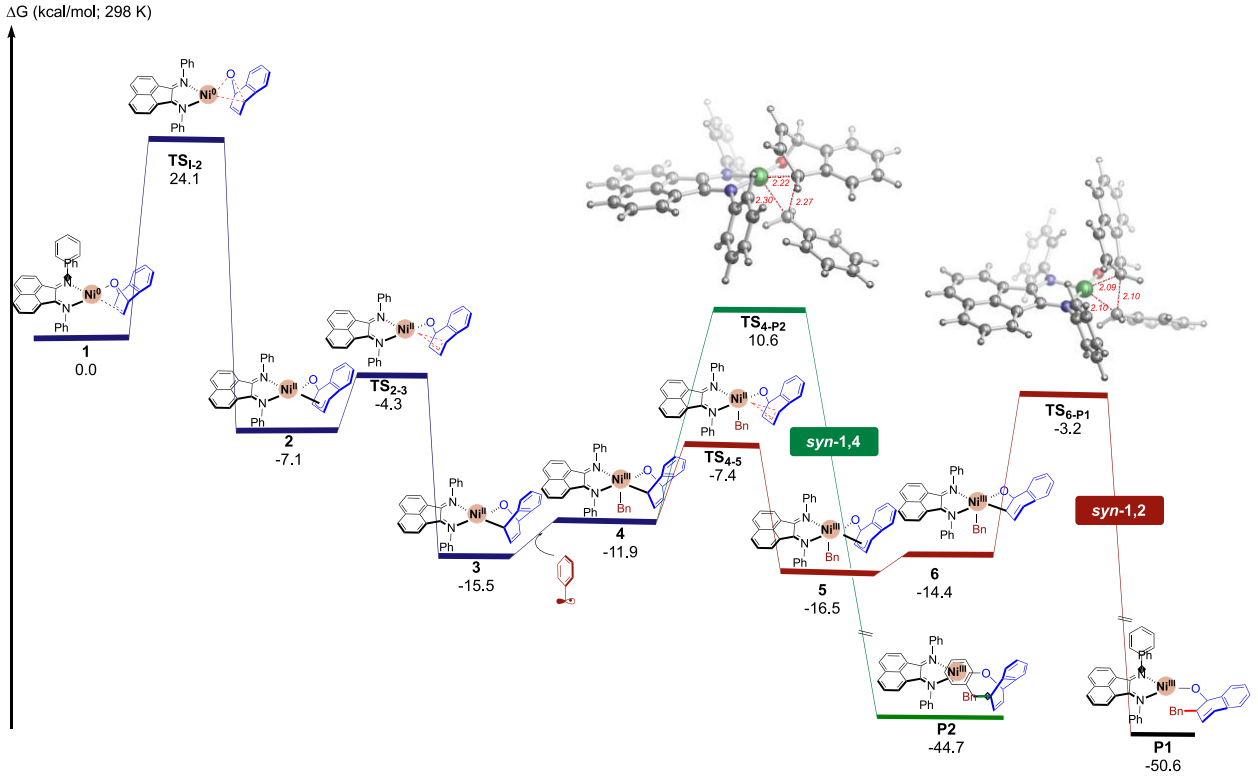

Figure 3. Energetics of the lowest energy pathway. Free energies (kcal/mol) are computed at the UM06/6-311+G(d,p)-CPCM(acetone)//UB3LYP-D3/6-31G(d)-CPCM(acetone) level of theory.

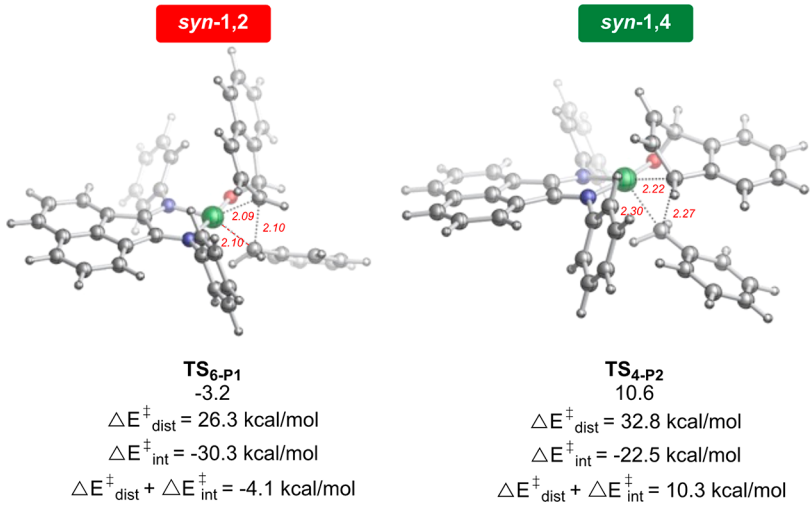

Figure 4. Distortion-interaction analysis of **TS-6-P1** and **TS-4-P2**. Energies (kcal/mol) are computed at the UM06/6-311+G(d,p)-CPCM(acetone)//UB3LYP-D3/6-31G(d)-CPCM(acetone) level of theory. The favorable interaction energy in **TS-6-P1** leads to the observed regioselectivity.

reaction with substrate **1a** and an equimolar mixture of DHPs **2l** and **2i** was performed. Upon completion and analysis of the reaction, the crude mixture showed a negligible preference for the para-fluorosubstituted product, thus indicating that, most likely, the benzyl residue is not involved in the product-determining step.

Density functional theory [UM06/6-311+G(d,p)-CPCM-(acetone)//UB3LYP-D3/6-31G(d)-CPCM(acetone)] was used to gain insights into the mechanism and factors controlling regioselectivity. For simplicity, only the lowest energy pathway is discussed (see the Supporting Information for competing pathways).[27] As shown in Figure 3, *syn* complexation of the epoxynaphthalene to the Ni(0) complex **1** allows direct oxidative addition to the C−O bond via **TS-1-2** (overall barrier is 24.1 kcal/mol) to form a Ni-O-π-allyl complex **2** (exergonic by 7.1 kcal/mol). In turn, this intermediate favors a low barrier $\pi-\sigma$ rearrangement (via **TS-2-3**), leading to the 1,4-Ni(II)-O-alkyl complex **3**. At this stage, the benzyl radical, presumably generated from the photocatalytic cycle (not calculated), will add to the Ni(II) intermediate **3**, leading to formation of Ni(III) complex **4**. Despite various attempts, the transition state could not be

DOI: 10.1021/acscatal.9b02458
ACS Catal. 2019, 9, 8835−8842

located for radical addition at this level of theory. Analysis of relaxed scans of the forming Ni−C bond[28−31] (see the Supporting Information for details) revealed a barrierless interconversion between **3** and **4**, while calculations optimized in the gas phase revealed a small energetic barrier (ca. 3 kcal/mol) between these two species (see the Supporting Information). Importantly, from this Ni(III) complex **4** intermediate, two pathways were found that could lead to the formation of the 1,4- and 1,2 products. As shown in the green pathway, Ni(III) intermediate **4** could undergo direct reductive elimination (via **TS-4-P2**) to form the 1,4-product (after protonation; not calculated) with an overall barrier of ∼26 kcal/mol from **3**. Although the barrier is reasonable, the formation of the 1,2-product (red) is significantly lower in energy. Specifically, **4** will preferentially undergo a facile $\sigma-\pi-\sigma$ isomerization (barrier is only ∼5 kcal/mol via **TS-4-5**), leading to the more energetically favored π-allyl Ni(III) **5** intermediate. In turn, this π-allyl intermediate will then form the 1,2-Ni(III) intermediate **6**, which is poised to undergo facile (barrier is ∼11 kcal/mol) reductive elimination via **TS-6-P1**, leading to the experimentally observed 1,2-*syn* product **P1** (after protonation; not calculated).

The distortion-interaction model[32] was used to explore the regioselectivity of the reaction. Specifically, we analyzed **TS-6-P1** and **TS-4-P2** (Figure 4). $\Delta E_{dist}^{\ddagger}$ is the energy required to distort intermediate **3** and the benzyl radical into the transition state geometry. $\Delta E_{int}^{\ddagger}$ is the energy of the interaction between the distorted fragments. The distortion energy of **TS-4-P2** is higher than that of **TS-6-P1** (∼7 kcal/mol), indicating that it takes more energy for intermediate **3** and the benzyl radical to distort into the transition state geometry required by **TS-4-P2** than by **TS-6-P1**, contributing to the overall higher energy of this transition state. Furthermore, the interaction energy between the distorted intermediate **3** and benzyl radical fragments in **TS-6-P1** is 8 kcal/mol lower than that in **TS-4-P2**. This result indicates that **TS-6-P1** has a more favorable interaction energy, leading to the observed 1,2-regioselectivity. It is worth noting that the C−C bond length between the benzyl radical and the epoxynaphthalene substrate in **TS-6-P1** is shorter (2.1 Å) than the same bond length in **TS-4-P2** (2.27 Å), indicating that **TS-6-P1** is a more dissociative transition state, which contributes to the more favorable interaction energy in **TS-6-P1**. Overall, the distortion-interaction model offers insight into the preference for the 1,2-product, as observed experimentally.

Overall, favorable *exo*-coordination [via Ni(0) **1**] dictates the *syn*-selectivity, whereas the exclusive 1,2-regioselectivity observed arises from a Curtin−Hammett scenario,[33] owing to a rapid $\sigma-\pi-\sigma$ isomerization that interconverts benzyl radical/Ni(II), σ-Ni(III), and π-allyl Ni(III) intermediates (**3**, **4**, **5**, and **6**) prior to undergoing regio-determining reductive elimination. The previously reported mechanism under palladium catalysis[15] (i.e., carbometalation followed by a β-oxygen elimination) would be unlikely for this system because, to the best of our knowledge, there is no precedent in the literature for a β-oxygen elimination with nickel. Indeed, computations predict this pathway to be unfavorable because of the high energy of the *syn* carbometalation transition state (see the Supporting Information for details).

CONCLUSION

In summary, taking advantage of the inherent mild reaction conditions of nickel/photoredox dual catalysis, the first general and efficient regio- and diastereoselective alkylation of oxa- and azabenzonorbornadienes has been developed. This new approach tolerates an array of functional groups and complex alkyl motifs, including saccharyl units, thus allowing the synthesis of arylated C-glycosyl antibiotic precursors. Mechanistic studies unraveled a new mechanistic paradigm, invoking a Ni(0) oxidative addition to form an π-allylnickel complex, followed by radical addition to generate a Ni(III) species, which under Curtin−Hammett conditions undergoes preferential reductive elimination from the 1,2-nickel adduct, resulting in complete regiocontrol.

ASSOCIATED CONTENT

Supporting Information

The Supporting Information is available free of charge on the ACS Publications website at DOI: 10.1021/acscatal.9b02458.

$C_{15}H_{18}O_2$ (CIF)

$C_{21}H_{29}NO_2$ (CIF)

Optimization data, experimental procedures, characterization data, NMR spectra, X-ray data, and DFT details (PDF)

AUTHOR INFORMATION

Corresponding Authors

*E-mail: gmolandr@sas.upenn.edu.

*E-mail: ogs@umd.edu.

ORCID

Youran Luo: 0000-0002-8033-2472

Jennifer K. Matsui: 0000-0003-0693-0404

Madeline E. Rotella: 0000-0002-7973-2452

Osvaldo Gutierrez: 0000-0001-8151-7519

Gary A. Molander: 0000-0002-9114-5584

Notes

The authors declare no competing financial interest.

ACKNOWLEDGMENTS

The authors are grateful for the financial support provided by NIGMS (R35 GM 131680 to G.A.M.) and NSF (CAREER, 1751568 to O.G.). Y.L. is grateful to the Wuyuzhang Honors College, Sichuan University for the financial support. O.G. is grateful to the University of Maryland College Park for start-up funds and computational resources from UMD Deepthought2 and MARCC/BlueCrab HPC clusters and XSEDE (CHE160082 and CHE160053).

REFERENCES

(1) (a) Nicolaou, K. C. The Emergence and Evolution of Erganic synthesis and why it is Important to Sustain it as an Advancing Art and Science for its own Sake. *Isr. J. Chem.* **2018**, *58*, 104−113. (b) Blakemore, D. C.; Castro, L.; Churcher, I.; Rees, D. C.; Thomas, A. W.; Wilson, D. M.; Wood, A. Organic Synthesis Provides Opportunities to Transform Drug Discovery. *Nat. Chem.* **2018**, *10*, 383−394. (c) Nicolaou, K. C.; Hale, C. R. H.; Nilewski, C.; Ioannidou, H. A. Constructing Molecular Complexity and Diversity: Total Synthesis of Natural Products of Biological and Medicinal Importance. *Chem. Soc. Rev.* **2012**, *41*, 5185−5238. (d) Smith, K.; Evans, D. A.; El-Hiti, G. A. Role of Modern Chemistry in Sustainable Arable Crop Protection. *Philos. Trans. R. Soc., B* **2008**, *363*, 623−637. (e) Baumgarten, M.; Bunz, U.; Müllen, K. Organic Synthesis and Materials Science. In *Molecular Engineering for Advanced Materials*; NATO ASI Series (Series C: Mathematical and Physical Sciences); Becher, J., Schaumburg, K., Eds.; Springer: Dordrecht, 1995; vol *456*.

DOI: 10.1021/acscatal.9b02458
ACS Catal. 2019, 9, 8835−8842

(2) (a) Brown, D. G.; Boström, J. Analysis of Past and Present Synthetic Methodologies on Medicinal Chemistry: Where Have All the New Reactions Gone? *J. Med. Chem.* **2016**, *59*, 4443−4458. (b) Hayler, J. D.; Leahy, D. K.; Simmons, E. M. A Pharmaceutical Industry Perspective on Sustainable Metal Catalysis. *Organometallics* **2019**, *38*, 36−46. (c) Boström, J.; Brown, D. G.; Young, R. J.; Keserü, G. M. Expanding the Medicinal Chemistry Synthetic Toolbox. *Nat. Rev. Drug Discovery* **2018**, *17*, 709−727.

(3) (a) Lovering, F.; Bikker, J.; Humblet, C. Escape From Flatland: Increasing Saturation as an Approach to Improving Clinical Success. *J. Med. Chem.* **2009**, *52*, 6752−6756. (b) Dandapani, S.; Marcaurelle, L. A. Accessing New Chemical Space for 'Undruggable' Targets. *Nat. Chem. Biol.* **2010**, *6*, 861−863.

(4) (a) Johansson Seechurn, C. C. C.; Kitching, M. O.; Colacot, T. J.; Snieckus, V. Palladium-Catalyzed Cross-Coupling: A Historical Contextual Perspective to the 2010 Nobel Prize. *Angew. Chem., Int. Ed.* **2012**, *51*, 5062−5085. (b) Gildner, P. G.; Colacot, T. J. Reactions of the 21st Century: Two Decades of Innovative Catalyst Design for Palladium-Catalyzed Cross-Couplings. *Organometallics* **2015**, *34*, 5497−5508. (c) Jana, R.; Pathak, T. P.; Sigman, M. S. Advances in Transition Metal (Pd, Ni, Fe)-Catalyzed Cross-Coupling Reactions using Alkyl-Organometallics as Reaction Partners. *Chem. Rev.* **2011**, *111*, 1417−1492.

(5) (a) Prier, C. K.; Rankic, D. A.; MacMillan, D. W. C. Visible Light Photoredox Catalysis with Transition Metal Complexes: Applications in Organic Synthesis. *Chem. Rev.* **2013**, *113*, 5322−5363. (b) Tellis, J. C.; Kelly, C. B.; Primer, D. N.; Jouffroy, M.; Patel, N. R.; Molander, G. A. Single-Electron Transmetalation via Photoredox/Nickel Dual Catalysis: Unlocking a New Paradigm for sp^3-sp^2 Cross-Coupling. *Acc. Chem. Res.* **2016**, *49*, 1429−1439. (c) Matsui, J. K.; Lang, S. B.; Heitz, D. R.; Molander, G. A. Photoredox-Mediated Routes to Radicals: The Value of Catalytic Radical Generation in Synthetic Methods Development. *ACS Catal.* **2017**, *7*, 2563−2575.

(6) For selected examples, see: (a) Johnston, C. P.; Smith, R. T.; Allmendinger, S.; MacMillan, D. W. C. Metallophotoredox-Catalysed sp3-sp3 Cross-Coupling of Carboxylic Acids with Alkyl Halides. *Nature* **2016**, *536*, 322−325. (b) Smith, R. T.; Zhang, X.; Rincon, J. A.; Agejas, J.; Mateos, C.; Barberis, M.; Garcia-Cerrada, S.; de Frutos, O.; MacMillan, D. W. C. Metallophotoredox-Catalyzed Cross-Electrophile Csp3-Csp3 Coupling of Aliphatic Bromides. *J. Am. Chem. Soc.* **2018**, *140*, 17433−17438. (c) Matsui, J. K.; Gutiérrez-Bonet, Á.; Rotella, M.; Alam, R.; Gutierrez, O.; Molander, G. A. Photoredox/Nickel-Catalyzed Single-Electron Tsuji-Trost Reaction: Development and Mechanistic Insights. *Angew. Chem., Int. Ed.* **2018**, *57*, 15847−15851.

(7) (a) Rayabarapu, D. K.; Cheng, C.-H. New Catalytic Reactions of Oxa- and Azabicyclic Alkenes. *Acc. Chem. Res.* **2007**, *40*, 971−983. (b) Lautens, M.; Fagnou, K.; Hiebert, S. Transition Metal-Catalyzed Enantioselective Ring-Opening Reactions of Oxabicyclic Alkenes. *Acc. Chem. Res.* **2003**, *36*, 48−58.

(8) (a) Chen, C.; Martin, S. F. Facile Synthesis of 2-Substituted 1,2-Dihydro-1-Daphthols and 2-Substituted 1-Napthols. *Org. Lett.* **2004**, *6*, 3581−3584. (b) Chen, C.-L.; Martin, S. F. Pd-Catalyzed Ring Opening of Oxa- and Azabicylic Alkenes with Aryl and Vinyl Halides: Efficient Entry to 2-Substituted 1,2-Dihydro-1-Napthols and 2-Substituted 1-Naphthols. *J. Org. Chem.* **2006**, *71*, 4810−4817.

(9) (a) Kaelin, D. E., Jr.; Lopez, O. D.; Martin, S. F. General Strategies for the Synthesis of the Major Classes of *C*-Aryl Glycosides. *J. Am. Chem. Soc.* **2001**, *123*, 6937−6938. (b) Kitamura, K.; Ando, Y.; Matsumoto, T.; Suzuki, K. Total Synthesis of Aryl *C*-Glycoside Natural Products: Strategies and Tactics. *Chem. Rev.* **2018**, *118*, 1495−1598. (c) Martin, S. F. Unified Strategy for the Synthesis of *C*-Aryl Glycosides. *Pure Appl. Chem.* **2003**, *75*, 63−70.

(10) Reynolds, A. J.; Scott, A. J.; Turner, C. I.; Sherburn, M. S. The Intramolecular Carboxyarylation Approach to Podophyllotoxin. *J. Am. Chem. Soc.* **2003**, *125*, 12108−12109.

(11) Yoshida, K.; Toyoshima, T.; Akashi, N.; Imamoto, T.; Yanagisawa, A. Rapid Screening for Asymmetric Catalysts: the Efficient Connection of Two Different Catalytic Asymmetric Reactions. *Chem. Commun.* **2009**, 2923−2925.

(12) Tsoung, J.; Krämer, K.; Zajdlik, A.; Liébert, C.; Lautens, M. Diastereoselective Friedel-Crafts Alkylation of Hydronaphthalenes. *J. Org. Chem.* **2011**, *76*, 9031−9045.

(13) (a) Goetz, A. E.; Shah, T. K.; Garg, N. K. Pyridynes and Indolynes as Building Blocks for Functionalized Heterocycles and Natural Products. *Chem. Commun.* **2015**, *51*, 34−45. (b) Chen, Q.; Yu, H.; Xu, Z.; Lin, L.; Jiang, X.; Wang, R. Development and Application of *o*-(Trimethylsilyl)aryl Fluorosulfates for the Synthesis of Arynes. *J. Org. Chem.* **2015**, *80*, 6890−6896. (c) Luo, R.; Liao, J.; Xie, L.; Tang, W.; Chan, A. S. C. Asymmetric Ring-Opening of Oxabenzonorbornadiene with Amines Promoted by a Chiral Iridium-Monophosphine Catalyst. *Chem. Commun.* **2013**, *49*, 9959−9961.

(14) Caple, R.; Chen, G. M.-S.; Nelson, J. D. The Addition of Butyllithiums to Benzonorbornadiene and 1,4-Dihydronaphthalene 1,4-*endo*-Oxide. *J. Org. Chem.* **1971**, *36*, 2874−2876. (b) Brown, N.; Luo, D.; Velde, D. V.; Yang, S.; Brassfield, A.; Buszek, K. R. Regioselective Diels-Alder Cycloadditions and Other Reactions of 4,5- 5,6- and 6,7-Indole Arynes. *Tetrahedron Lett.* **2009**, *50*, 63−65. (c) Buszek, K. R.; Luo, D.; Kondrashov, M.; Brown, N.; VanderVelde, D. Indole-Derived Arynes and their Diels-Alder Reactivity with Furans. *Org. Lett.* **2007**, *9*, 4135−4137. For a transformation using zirconium-based reagents, see: (d) Barluenga, J.; Rodríguez, F.; Álvarez-Rodrigo, L.; Zapico, J. M.; Fañanás, F. J. Zirconium-Mediated Coupling Reactions of Amines and Enol or Allyl Ethers: Synthesis of Allyl- and Homoallylamines. *Chem. - Eur. J.* **2004**, *10*, 109−116.

(15) For selected examples, see: (a) Lautens, M.; Renaud, J.-L.; Hiebert, S. Palladium-Catalyzed Enantioselective Alkylative Ring Opening. *J. Am. Chem. Soc.* **2000**, *122*, 1804−1805. (b) Lautens, M.; Hiebert, S.; Renaud, J.-L. Mechanistic Studies of the Palladium-Catalyzed Ring Opening of Oxabicyclic Alkenes with Dialkylzinc. *J. Am. Chem. Soc.* **2001**, *123*, 6834−6839. (c) Lautens, M.; Hiebert, S. Scope of Palladium-Catalyzed Alkylative Ring Opening. *J. Am. Chem. Soc.* **2004**, *126*, 1437−1447. (d) Cabrera, S.; Gomez Arrayas, R.; Carretero, J. C. Cationic Planar Chiral Palladium P,S Complexes as Highly Efficient Catalysts in the Enantioselective Ring Opening of Oxa- and Azabicyclic Alkenes. *Angew. Chem., Int. Ed.* **2004**, *43*, 3944−3947. (e) Li, M.; Yan, X.-Y.; Hong, W.; Zhu, X.-Z.; Cao, B.-X.; Sun, J.; Hou, X.-L. Palladium-Catalyzed Enantioselective Ring Opening of Oxabicyclic Alkenes with Organozinc Halides. *Org. Lett.* **2004**, *6*, 2833−2835. (f) Cabrera, S.; Arrayás, R. G.; Alonso, I.; Carretero, J. C. Fesulphos-Palladium(II) Complexes as Well-Defined Catalysts for Enantioselective Ring Opening of Meso Heterobicyclic Alkenes with Organozinc Reagents. *J. Am. Chem. Soc.* **2005**, *127*, 17938−17947.

(16) (a) Wu, M.-S.; Jeganmohan, M.; Cheng, C.-H. A Highly Regio- and Stereoselective Nickel-Catalyzed Ring-Opening Reaction of Alkyl- and Allylzirconium Reagents to 7-Oxabenzonorbornadienes. *J. Org. Chem.* **2005**, *70*, 9545−9550. (b) Ladjel, C.; Fuchs, N.; Zhao, J.; Bernardinelli, G.; Alexakis, A. New Bifunctional Substrates for Copper-Catalyzed Asymmetric Conjugate Addition Reactions with Trialkylaluminum. *Eur. J. Org. Chem.* **2009**, *2009*, 4949−4955. (c) Huang, Y.; Ma, C.; Lee, Y. X.; Huang, R.-Z.; Zhao, Y. Cobalt-Catalyzed Allylation of Heterobicyclic Alkenes: Ligand-Induced Divergent Reactivities. *Angew. Chem., Int. Ed.* **2015**, *54*, 13696−13700.

(17) (a) Bertozzi, F.; Pineschi, M.; Macchia, F.; Arnold, L. A.; Minnaard, A. J.; Feringa, B. L. Copper Phosphoramidite Catalyzed Enantioselective Ring-Opening of Oxabicyclic Alkenes: Remarkable Reversal of Stereocontrol. *Org. Lett.* **2002**, *4*, 2703−2705. (b) Arrayás, R. G.; Cabrera, S.; Carretero, J. C. Copper-Catalyzed Anti-Stereocontrolled Ring Opening of Oxabicyclic Alkenes with Grignard Reagents. *Org. Lett.* **2003**, *5*, 1333−1336. (c) Zhang, W.; Wang, L.-X.; Shi, W.-J.; Zhou, Q.-L. Copper-Catalyzed Asymmetric Ring Opening of Oxabicyclic Alkenes with Grignard Reagents. *J. Org. Chem.* **2005**, *70*, 3734−3736. (d) Zhang, W.; Zhu, S.-F.; Qiao, X.-C.; Zhou, Q.-L. Highly Enantioselective Copper-Catalyzed Ring Opening of Oxabicyclic Alkenes with Grignard Reagents. *Chem. - Asian J.* **2008**, *3*, 2105−2111. (e) Bos, P. H.; Rudolph, A.; Pérez, M.; Fañanás-Mastral,

DOI: 10.1021/acscatal.9b02458
ACS Catal. 2019, 9, 8835−8842

M.; Harutyunyan, S. R.; Feringa, B. L. Copper-Catalyzed Asymmetric Ring Opening of Oxabicyclic Alkenes with Organolithium Reagents. *Chem. Commun.* **2012**, *48*, 1748−1750.
(18) (a) Duan, J.-P.; Cheng, C.-H. Palladium-Catalyzed Reductive Coupling of Organic Halides with 7-Heteroatom Norbornadienes. New Synthetic Methods for Substituted Aryls and *cis*-1,2-Dihydro-1-Naphthyl Alcohols and Carbamates. *Organometallics* **1995**, *14*, 1608−1618. (b) Parthasarathy, K.; Jeganmohan, M.; Cheng, C.-H. Palladium-Catalyzed Multistep Reactions Involving Ring Closure of 2-Iodophenoxyallenes and Ring Opening of Bicyclic Alkenes. *Org. Lett.* **2006**, *8*, 621−623. (c) Li, Y.; Chen, J.; He, Z.; Qin, H.; Zhou, Y.; Khan, R.; Fan, B. Cobalt-Catalyzed Asymmetric Reactions of Heterobicyclic Alkenes with *in situ* Generated Organozinc Halides. *Org. Chem. Front.* **2018**, *5*, 1108−1112.
(19) Shukla, P.; Sharma, A.; Pallavi, B.; Cheng, C.-C. Nickel-Catalyzed Reductive Heck Type Coupling of Saturated Alkyl Halides with Acrylates and Oxabenzonorbornadiene. *Tetrahedron* **2015**, *71*, 2260−2266.
(20) For other nonorganometallic nucleophiles, see: (a) Loh, C. C. J.; Schmid, M.; Peters, B.; Fang, X.; Lautens, M. Exploiting Distal Reactivity of Coumarins: A Rhodium-Catalyzed Vinylogous Asymmetric Ring-Opening Reaction. *Angew. Chem., Int. Ed.* **2016**, *55*, 4600−4604. (b) Zhang, L.; Le, C. M.; Lautens, M. The Use of Silyl Ketene Acetals and Enol Ethers in the Catalytic Enantioselective Ring Opening of Oxa/Aza Bicyclic Alkenes. *Angew. Chem., Int. Ed.* **2014**, *53*, 5951−5954. (c) Yang, J.; Sekiguchi, Y.; Yoshikai, N. Cobalt-Catalyzed Enantioselective and Chemodivergent Addition of Cyclopropanols to Oxabicyclic Alkenes. *ACS Catal.* **2019**, *9*, 5638−5644.
(21) (a) Gutiérrez-Bonet, Á.; Tellis, J. C.; Matsui, J. K.; Vara, B. A.; Molander, G. A. 1,4-Dihydropyridines as Alkyl Radical Precursors: Introducing the Aldehyde Feedstock to Nickel/Photoredox Dual Catalysis. *ACS Catal.* **2016**, *6*, 8004−8008. (b) Gutiérrez-Bonet, Á.; Remeur, C.; Matsui, J. K.; Molander, G. A. Late-Stage C-H Alkylation of Heterocycles and 1,4-Quinones via Oxidative Homolysis of 1,4-Dihydropyridines. *J. Am. Chem. Soc.* **2017**, *139*, 12251−12258. (c) Dumoulin, A.; Matsui, J. K.; Gutiérrez-Bonet, Á.; Molander, G. A. Synthesis of Non-Classical Arylated *C*-Saccharides through Nickel/Photoredox Dual Catalysis. *Angew. Chem., Int. Ed.* **2018**, *57*, 6614−6618.
(22) (a) Lautens, M.; Ma, S. Nickel-Catalyzed Addition of Grignard Reagents to Oxabicyclic Compounds. Ring-Opening Reactions with Previously Unreactive Substrates and Nucleophiles. *J. Org. Chem.* **1996**, *61*, 7246−7247. (b) Loh, C. C. J.; Fang, X.; Peters, B.; Lautens, M. Benzylic Functionalization of Anthrones via the Asymmetric Ring Opening of Oxabicyclic Utilizing a Fourth-Generation Rhodium Catalytic System. *Chem. - Eur. J.* **2015**, *21*, 13883−13887.
(23) A vast array of chiral ligands was tested (phosphines, bisoxazilindes, etc.) to achieve enantiocontrol via a desymmetrization strategy. Note, reactivity decreased significantly or was completely halted, and no enantiocontrol was observed in any case. We believe that, in the cases where reactivity was observed, a ligandless-catalytic system was responsible, hence the lack of enantioenriched product formation.
(24) It has been reported that DHPs undergo quantitative homolysis in the presence of catalytic amounts of 4CzIPN through a radical chain process. See ref 21a.
(25) Sgro, M. J.; Stephan, D. W. Synthesis and Exchange Reactions of Ni-Dimine-COD, Acetylene and Olefin Complexes. *Dalton Trans.* **2010**, *39*, 5786−5794.
(26) Hansch, C.; Leo, A.; Taft, R. W. A Survey of Hammett Substituent Constants and Resonance and Field Parameters. *Chem. Rev.* **1991**, *91*, 165−195.
(27) Gutierrez, O.; Tellis, J. C.; Primer, D. N.; Molander, G. A.; Kozlowski, M. C. Nickel-Catalyzed Cross-Coupling of Photoredox Generated Radicals: Uncovering a General Manifold for Stereoconvergence in Nickel-Catalyzed Cross-Couplings. *J. Am. Chem. Soc.* **2015**, *137*, 4896−4899.
(28) Kaur, R.; Vikas. Conflict in the Mechanism and Kinetics of the Barrierless Reaction between SH and NO_2 Radicals. *J. Phys. Chem. A* **2018**, *122*, 1926−1937.
(29) Wenthold, P. G.; Winter, A. H. Nucleophilic Addition to Singlet Diradicals: Homosymmetric Diradicals. *J. Org. Chem.* **2018**, *83*, 12390−12396.
(30) Breitenfeld, J.; Wodrich, M. D.; Hu, X. Bimetallic Oxidative Addition in Nickel-Catalyzed Alkyl−Aryl Kumada Coupling Reactions. *Organometallics* **2014**, *33*, 5708−5715.
(31) de Aguirre, A.; Funes-Ardoiz, I.; Maseras, F. Four Oxidation States in a Single Photoredox Nickel-Based Catalytic Cycle: A Computational Study. *Angew. Chem., Int. Ed.* **2019**, *58*, 3898−3902.
(32) Bickelhaupt, F. M.; Houk, K. N. Analyzing Reaction Rates with the Distortion/Interaction-Activation Strain Model. *Angew. Chem., Int. Ed.* **2017**, *56*, 10070−10086.
(33) Seeman, J. I. Effect of conformational change on reactivity in organic chemistry. Evaluations, applications, and extensions of Curtin-Hammett/Winstein-Holness kinetics. *Chem. Rev.* **1983**, *83*, 83−134.

DOI: 10.1021/acscatal.9b02458
ACS Catal. 2019, 9, 8835−8842